Variation of Effective Input Motions to Superstructure Based on Long Term Earthquake Observation

M. Kawashima
Sumitomo Mitsui Construction Co. Ltd, Japan

M. Iguchi
Tokyo University of Science, Japan

T. Kashima
Building Research Institute, Japan

SUMMARY:
Characteristics of effective input motions to a structure that include the effects of SSI are extracted and discussed based on results for 86 seismic events observed for 14 years with emphasis on the effect of rocking input motion. The results include for the extensive records of main and aftershocks of the Tohoku Earthquake in 2011.

Keywords: Soil-Structure Interaction, Effective Input Motion, Earthquake Observation, Composite Response Spectrum

1. INTRODUCTION

Since the pioneering work of Housner (1957) and Yamahara (1970), it has been widely recognized that earthquake input motions to a superstructure are different from those recorded on the soil surface at the site. To clarify how the earthquake ground motions are modified when being inputted to a superstructure becomes essential in the simulation analyses of seismic responses of a building as well as in assessment of seismic resistant capacity of a structure. The foundation response during earthquakes, which includes the effects of inertial and kinematic interactions, becomes the actual input motion to superstructure and is referred to as an effective input motion (EIM). One of the significant points to be noted is rotational components to act as input motions to superstructure in addition to translational motion. Though the subject concerning the EIM should be more highlighted, the evaluation of EIM based on real earthquake observations has been few presented.
In the past studies of evaluation of the EIM, simple indices have been used, such as a ratio between the peak acceleration motions on the foundation (PFA) and on the ground (PGA). Yasui et al. (1998) revealed 30% reduction of the EIM for a horizontal component with use of the peak ratio PFA/PGA by analyzing seismic records observed in the heavily damaged area during the 1995 Hyogoken-Nanbu earthquake in Kobe Japan. Iguchi et al. (2000) indicated that the reduction of EIM is significantly dependent on the frequency component included in the surface ground motions. Kojima et al. (2004) studied a reduction effect or input loss of earthquake motions comparing with the ground motions for various structures with different embedded depth of foundation and with different size. Stewart et al. (1998), on the other hand, evaluated EIM with an index of response spectrum ratio of 5% damping for the seismic motions recorded on the foundation and on the soil surface. Kawashima et al. (2007) introduced a new index defined as a ratio of the square root of an integrated-squared motion (SRISM) observed on the foundation to that on the soil surface. In the study, the effectiveness of the index was confirmed with earthquake records observed on a large shaking table foundation and at the site.
This paper discusses characteristics of EIM extracted from earthquake observations in and around an annex building of Building Research Institute (BRI) at Tsukuba Japan for these fourteen years. Among the observed data, records of the latest great earthquakes of the North East Pacific Japan Earthquake on 11th of March, 2011 and its aftershocks are included.
Regarding the annex building, it was found that the dynamic characteristics of the building have been showing a remarkable change with the passage of time over years (Kashima et al. (2006)). This fact enables us to study the effect of buildings with the same foundation and soil deposit but having

different dynamic characteristics of a structure on EIM. In evaluation of EIM, an index defined as a ratio of the square root of an integrated-squared motion (SRISM) observed on the foundation to that on the soil surface is used instead of conventionally used peak ratio or spectral ratio. This paper studies the EIM focusing on the following points. (1) To elucidate parameters that might affect essentially on EIM, such as frequency components included in the ground motions, magnitude of ground motions, dynamic characteristics of the building, and so forth. (2) To investigate the effects of aging of the building on EIM. (3) To confirm the effectiveness of the SRISM index for the building. (4) To discuss the effect of rotational component of EIM on the response of superstructure with introducing newly defined composite response spectra.

2. OUTLINE OF OBSERVATION SYSTEM

2.1 BRI Annex Building and Sites

Continuous earthquake observation has been conducted in Building Research Institute (BRI) of Japan since 1950s. The BRI annex building is one of the stations of the BRI strong motion network, and a large number of earthquake records have been observed with accelerometers densely installed within the building as well as in the surrounding soil (Kashima et al. 2006).

The annex building is a steel-reinforced concrete framed structure with eight stories above ground and one story basement, and was completed in 1998. The external view of this building is shown in **Figure 2.1**. The building is supported by a flat mat foundation embedded 8.2m deep in the soil and has no pile. The annex building is connected to the main building with passage ways, but the two buildings are separated by expansion joint and are structurally independent. The soil under the basement mat is the cohesive soil of shear wave velocity 160m/sec. The engineering bedrock with shear wave velocity of about 500m/sec is underlying about 89m below the surface at this site.

Figure 2.1. External view of the BRI annex building

2.2 Seismic Observation System

The seismic observation system at BRI site is composed of 22 accelerometers installed in the annex building, at the site and some on the main building, and some are deployed so as to enable to extract the dynamic characteristics of soil-structure interaction effects. The configuration of the seismic observation system is shown in **Figure 2.2(a)**. Eleven accelerometers are installed in the annex building and seven in the surrounding soil. The observed record at the point A01 is selected as the reference point representing the surface ground motion at the site.

Three accelerometers are installed on both sides of the basement, which enable us to evaluate not only translational but also rotational (rocking and torsional) motions of the system.

Figure 2.2(b) shows the plan of the basement floor and locations of seismographs. Two accelerometers are deployed in the east and west sides of the fifth and second floors as shown in **Figure 2.2(a)**. In computing translational motions, floor responses were evaluated by averaging over

the whole records observed on the floor. Rigid-body rocking motions of the basement were evaluated by dividing the difference of vertical motions at both sides of foundation by the separation distance between the sensors. In this paper, the effects of torsional motions are not taken into account.

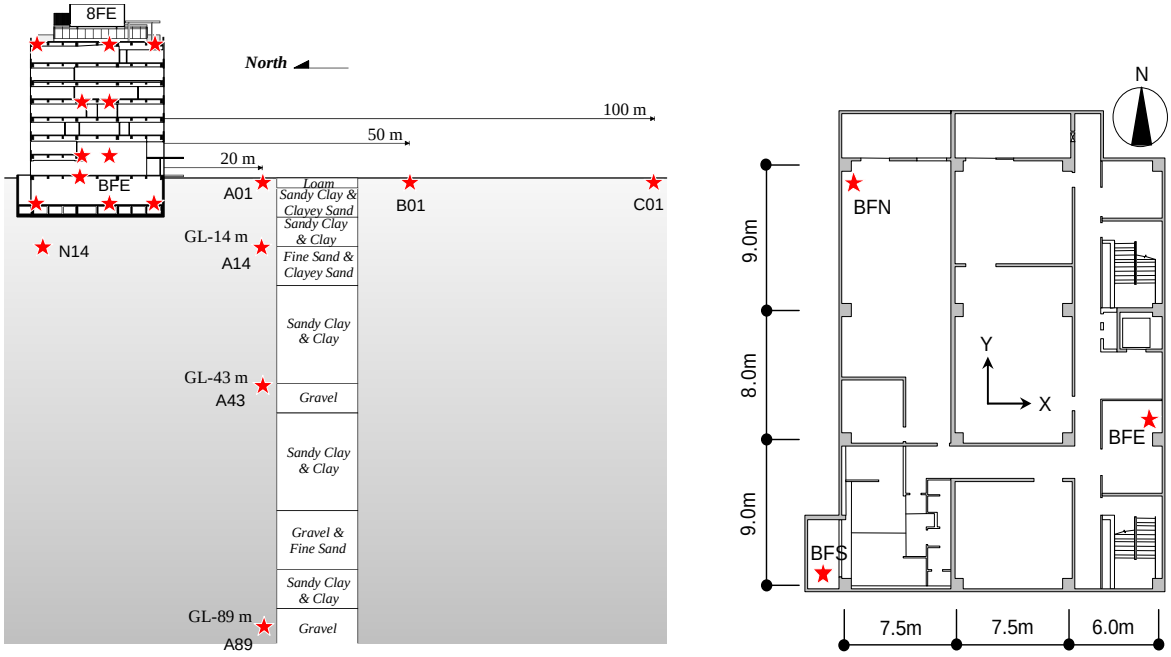

(a) Layout of seismometers in strucure and at the site. (b) Seismometers on basement.

Figure 2.2. Seismic observation system at BRI site

3. AN INDEX FOR EVALUATION OF EIM

In evaluation of the EIM, an index introduced by Kawashima et al. (2007) is used in this paper. The index was shown to have a close relation to the transfer function between the foundation response and the ground motion at the site. The effectiveness of the index has been also confirmed in the previous paper. More detail about the index may be found elsewhere (Kawashima et al. 2007)).
Letting $a_g(t)$ and $a_f^{\Delta}(t)$ be the time histories of acceleration recorded on the ground and on the foundation (translation), the index is defined as in Eqn. 3.1.

$$\alpha_a^{\Delta} = \frac{\sqrt{\int_0^T \left| a_f^{\Delta}(t) \right|^2}}{\sqrt{\int_0^T \left| a_g(t) \right|^2}} \tag{3.1}$$

In Eqn. (3.1), T denotes the duration of earthquake motions. Thus defined coefficient α_a^{Δ} expresses a ratio of the square root of integrated squared-motion (SRISM) on the ground to that observed on the foundation. We refer to α_a^{Δ} as an effective-input-coefficient (EIC) of a translational acceleration motion. In the same manner, the index for rotational component of EIM is defined as follow.

$$\alpha_a^{\Phi} = \frac{\sqrt{\int_0^T \left| L \cdot a_f^{\Phi}(t) \right|^2}}{\sqrt{\int_0^T \left| a_g(t) \right|^2}} \tag{3.2}$$

where $a_f^{\Phi}(t)$ is a time history of rocking angular acceleration motion of the foundation, and L denotes the reference length introduced to make α_a^{Φ} dimensionless. In this paper, L is set as L=1m.

4. RESULTS AND DISCUSSION

4.1 Variation of Dynamic Characteristics of Annex Building

On basis of records observed in this building and at the site for 14 years, the change in dynamic characteristics of the building has been studied in detail with different viewpoints (Kashima et al. (2006), Iguchi et al. (2010), and Kawashima et al. (2012). It was found that the fundamental frequency of the superstructure obtained excluding the effect of the soil flexibility has gradually decreased in both sides of the building. It is presumed that the change is attributed mainly to damage to non-structural elements and nonlinearity of the structural elements of superstructure for intermediate or rather extensive earthquake ground motions.

Figure 4.1 shows the change in the first mode frequency in the NS-direction for 14 years (1998 to 2011). The figure includes the results for main and aftershocks of the off the Pacific coast of Tohoku Earthquake in 2011. The size of circles plotted in this figure indicates the peak relative displacement of superstructure (PRDoS). Inspection of **Figure 4.1** reveals that the fundamental frequency has decreased from 1.9Hz to 1.4Hz before the Tohoku Earthquake in 2011. This corresponds to about 50% reduction of lateral stiffness of the superstructure. It will be also noticed that the change of the stiffness has become remarkable when the structure has experienced large deformation in superstructure. In particular, remarkable reduction of the first mode frequency is recognized during the short period of the Tohoku Earthquakes in 2011.

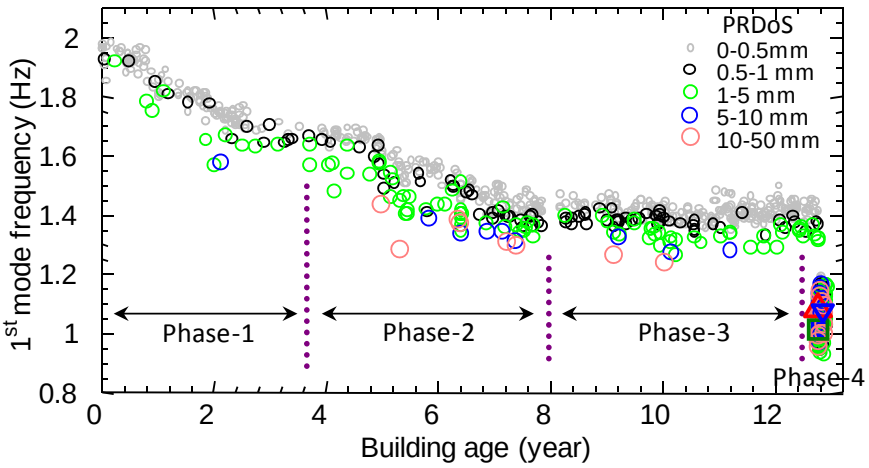

Figure 4.1. Change in fundamental frequency in the NS-direction with age of building

With consideration of the deteriorating trend shown in the results, the whole term of 14 years is sorted into four periods. Each period is referred to here as phase. Phase one corresponds to the term of four years after the completion of the building. Phase two is the successive term of about three and half years. In the meanwhile of the phase two, it has marked almost the same amount of change as in the phase one. Phase three is the term of four years exhibiting little change in the fundamental frequency. Finally, phase four corresponds to the short period of main shock and aftershocks of the Tohoku Earthquake.

4.2 Selection of Earthquake Data for Analyses

More than 950 sets of data have been recorded at the site for about 14 years including the aftershocks of the Tohoku Earthquake. Among the numerous data, the records exceeding 10 gals of peak ground acceleration (PGA) on the soil surface were chosen for the analyses. As a result, 86 sets of records were analysed in this paper. The profile of earthquake records selected for the analyses of EIM are listed in **Table 4**.1. The table summarizes the period corresponding to each phase, number of earthquakes, the maximum PGA on the soil surface and the mean value of PGAs in the respective phases. The average value of PGA in each phase was less than 30gals except the phase four. The maximum PGA at the site through the observations was 279.3gals that was recorded at the Tohoku Earthquake in 2011.

Table 4.1. Profile of Earthquake Data in Respective Phases

Phase	Period	No. of Eqs.	Max of PGA(A01)	PGA Average
Phase-1	98/ 6/ 4 - 02/ 7/13	17	74.3	24.1
Phase-2	02/10/21 - 06/ 2/ 1	30	54.5	21.3
Phase-3	07/ 5/ 8 - 10/11/ 5	23	49.6	22.2
Phase-4	11/ 3/11 - 11/ 4/26	16	279.3	66.3
			(cm/sec^2)	(cm/sec^2)

4.3 Observed Transfer Functions

The frequency characteristics of EIM can be observed through transfer function which is defined as a ratio of frequency response of the basement to the amplitude of the surface ground motion. The observed results of horizontal and rocking transfer functions for each phase are shown in **Figures 4.2 (a)** and **(b)**. As for the rocking transfer function, reference height is set as L=1m. In these figures mean values of transfer functions for the respective phases and average over the total 86 records are shown together with its $\pm\sigma$ of the standard deviation. Shown are the results in the NS-direction.

It will be noticed from **Figure 4.2 (a)** that the horizontal component tends to decrease with increase of frequency. The remarkable reduction in the horizontal component with increase of frequency is recognized. The reduction goes down to about 75% around 10Hz comparing with the ground surface motion. Similar tendency has been recognized for other foundation (Iguchi et al. (2004)).

It would be interesting to notice that as for the horizontal transfer function the reduction tendency is almost same irrespective of difference of phases. This indicates that the effect of stiffness of superstructure on the horizontal input motion is small and the transfer function is almost independent to magnitude of ground motions as far as this building is concerned.

In contrast, different characteristics may be recognized for rocking component as shown in **Figure 4.2 (b)**. The rocking component tends to increase up to about 7Hz and become almost constant for higher frequency. The effects of the difference of phase on the rocking transfer function are clearly seen around 1.5Hz. The peak values for the respective phases tend to be smaller and to shift to left as the phase moves from one to four which corresponds to reduction of horizontal stiffness of superstructure.

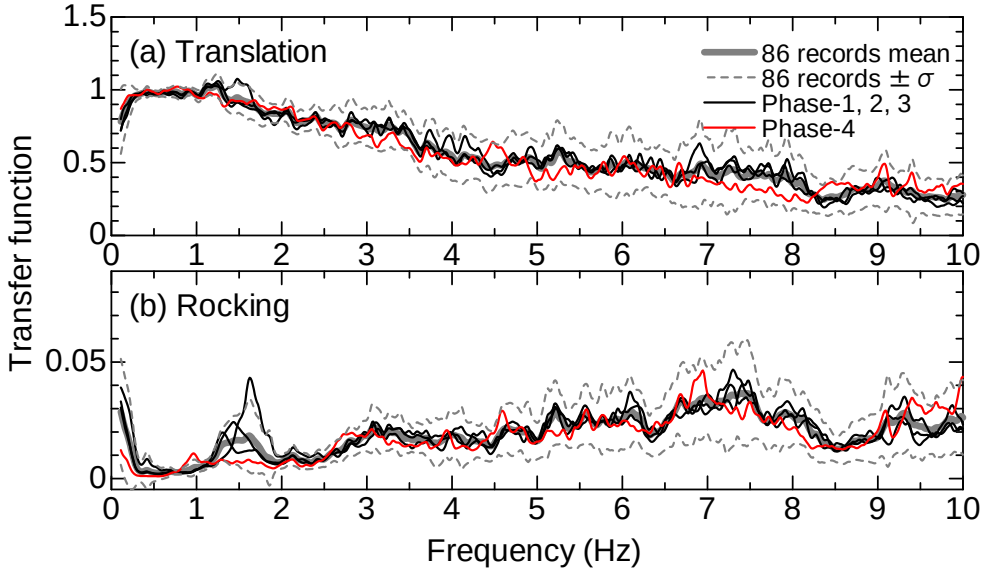

Figure 4.2. Observed average transfer functions of EIM of respective phases and the whole in the NS-direction

Comparing the peak frequencies with the results shown in **Figure 4.1**, it will be noticed that the peak frequencies correspond to the average frequencies for the respective phases. These tendencies may be explained by reduction of the additional rocking motion of foundation due to the action of overturning moment that would decrease with decrease of fundamental frequency of the structure.

Not showing in a figure, similar tendencies could be detected also in the EW-direction.

4.4 Comparison of Evaluation Indices of EIM with Transfer Functions

As mentioned earlier, in evaluation of EIM peak acceleration ratio between the foundation and the ground motions (PFA/PGA ratio) has been widely used for simplicity. Another alternative index (EIC) has been proposed by Kawashima et al. (2007). It would be worth comparing these indices with the observed transfer functions to see how these indices fit to the transfer functions. Compared results are shown in **Figure 4.3 (a)** and **(b)** for translational and rocking components, respectively. Plotted are the results evaluated by peak ratio and EIC defined in Eqns. (3.1) and (3.2). The corresponding results of transfer functions are those obtained by averaging the results of 86 earthquake records and its $\pm\sigma$. Marked by open triangle is the results of peak ratio, and open circle indicates the results of EIC.

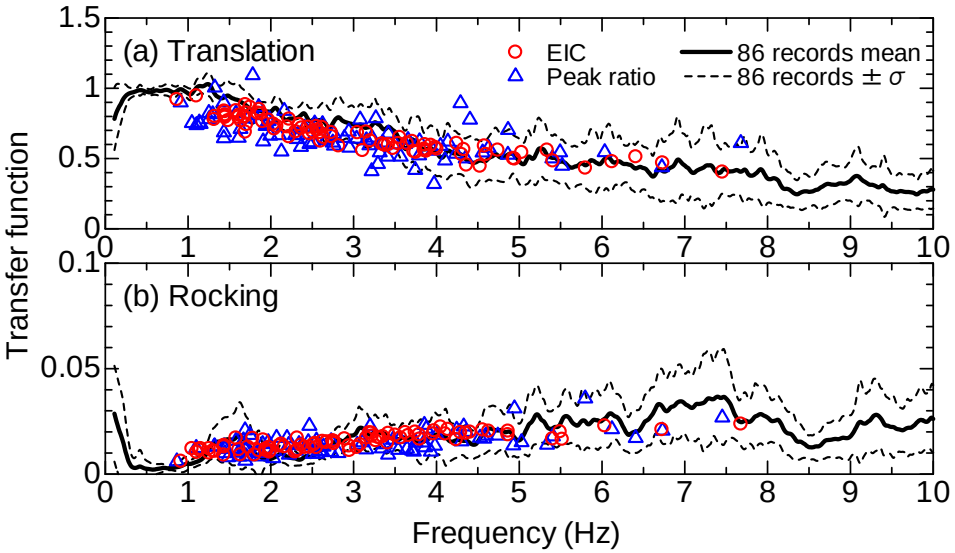

Figure 4.3. Comparison between observed average transfer functions and indices of EICs in the NS-direction

In plotting the results of indices, two equivalent predominant frequencies of the ground motions are introduced. One is the frequency defined by

$$f_{eq} = \frac{1}{2\pi} \cdot \sqrt{\frac{\int_{t_p - t_e}^{t_p + t_e} a_g{}^2(t)dt}{\int_{t_p - t_e}^{t_p + t_e} v_g{}^2(t)dt}} \tag{4.1}$$

where $v_g(t)$ and $a_g(t)$ are velocity and acceleration motions, respectively, on the soil surface, and t_p is the time that acceleration ground motion shows its peak and t_e is a time interval to obtain the average of the predominant frequency of the ground motion. As for the averaging time interval, t_e is set as 2sec. Thus, the f_{eq} is interpreted as a mean predominant frequency of ground motion around the peak amplitude of the motion. Another predominant frequency of the ground motion adopted in this paper is a simpler one evaluated based on the PGV/PGA ratio defined by

$$f_{peak} = \frac{1}{2\pi} \cdot \frac{PGA}{PGV} \tag{4.2}$$

The results of EIC are plotted at frequencies corresponding to f_{eq}, and on the other hand the results evaluated with the peak ratio (PFA/PGA) are plotted against f_{peak}.

It will be noticed from **Figure 4.3 (a)** and **(b)** that the evaluated results of EIC agree well with the observed transfer functions. In contrast, the results based on peak ratio vary widely from the mean of transfer functions. It may be concluded that the results evaluated by the peak ratio is less stable than the results evaluated using the EIC.

4.5 Analytical Estimation Result versus Observed Transfer Function

For estimation of the foundation input motion for embedded foundations, some numerical formulas have been proposed. In applying these estimation formulas, it should be reminded that most of the proposed formulas are presented for estimation of the foundation input motions. The foundation input motion which is defined as seismic response of a massless foundation differs from the effective input motion which includes the additional motions of foundation due to action of inertial forces of foundation and the superstructure. Since the foundation input motions cannot be extracted directly from observation and the effects of additional motion due to the inertial force may be considered to be small except the frequency around 1.5Hz, it would be meaningful to compare the results of foundation input motions based on the estimation formulas with observed transfer functions to see the applicability of the presented formulas.

An estimation formula is proposed by Harada et al. (1985) for both translational and rocking components of foundation input motion. For translational motion, it is express as

$$\frac{\Delta_H{}^*}{u_0} = \begin{cases} \left|\dfrac{\sin kh}{kh}\right| & 0 \le kh \le \pi/2 \\ 0.63 & \pi/2 \le kh \end{cases} \tag{4.3}$$

In which $\Delta_H{}^*$ is the horizontal foundation input motion defined on the foundation base, u_0 is horizontal ground motion at the site, h is the embedment depth of a foundation and $k=\omega/V_s$ is a wave number of the surrounding soil with shear wave velocity V_s. As for rocking foundation input motion, an estimation formula is provided as follows for embedment ratio h/a less than 1.0 (Harada et al. (1985)).

$$\frac{a\Phi^*}{u_0} = \begin{cases} 0.4(h/a)\left|1-\cos kh\right| & 0 \le kh \le \pi/2 \\ 0.4(h/a) & \pi/2 \le kh \end{cases} \tag{4.4}$$

In Eqn. (4.4) a is the equivalent radius of an embedded foundation, Φ^* is the rocking component of foundation input motion.

Another estimation formula for the horizontal foundation input motion has been presented by Subcommittee of Earthquake Engineering in Japan Society of Civil Engineering (1992) as follows.

$$\frac{\Delta_H{}^*}{u_0} = \begin{cases} \left(\dfrac{\sin kh}{kh}\right)^2 & 0 \le kh \le \pi/2 \\ 0.405 & \pi/2 \le kh \end{cases} \tag{4.5}$$

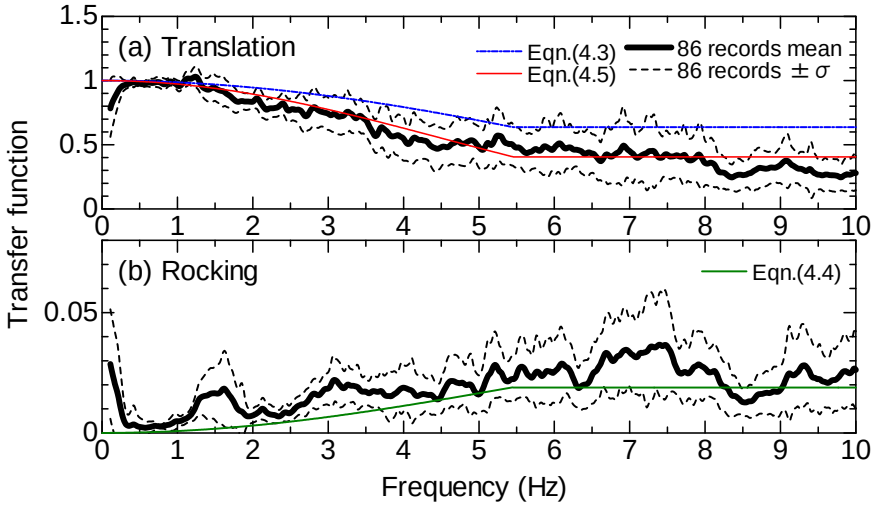

Figure 4.4. Comparison between observed transfer functions and results by estimation formulas

Compared results of observed transfer functions with those evaluated by the estimation formulas are shown in **Figure 4.4 (a)** and **(b)** for translational and rocking components, respectively. In applying Eqn. (4.4) to this building, the equivalent radius a is set as a=13.2m.
The computed results based on Eqns. (4.3) and (4.4) tend to overestimate for translational component and underestimate for rocking motion. The result estimated based on Eqn. (4.5), on the other hand, provides fairly excellent estimation for translational input motion.

4.6 Composite Response Spectrum

In seismic design of structures, the effect of rocking input motion has not been taken into account. This section is addressed to elucidate how the rocking input motion could affect on the total response of structures. In order to study the effects, it would be appropriate to investigate by means of the seismic response analysis of a one-mass-system subjected to simultaneous excitation of horizontal and rocking input motions. **Figure 4.5** shows a mathematical model of one-mass-system when excited by two components of input motions at the basement. We refer here the response spectrum of the one-mass-system subjected to both translational and rocking excitations as a composite response spectrum.

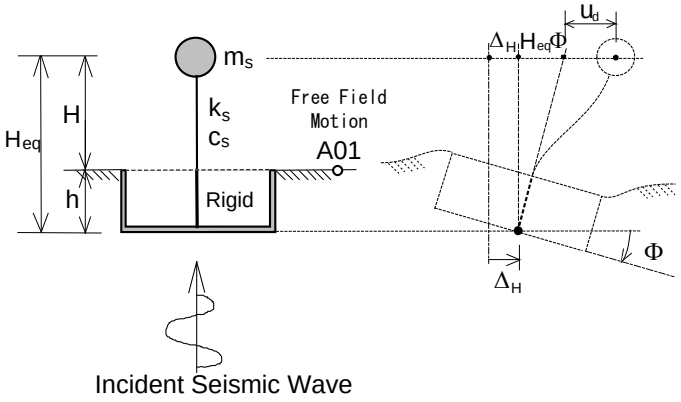

Figure 4.5. Mathematical model of one-mass-system subjected to translational and rocking input motions.

Referring to the model shown in **Figure 4.5**, the equation of motion can be expressed by Eqn. (4.6).

$$m_s\ddot{u}_d + c_s\dot{u}_d + k_s u_d = -m_s(\ddot{\Delta}_H + H_{eq}\ddot{\Phi}) \tag{4.6}$$

where m_s, c_s and k_s are the mass, damping coefficient and spring constant, respectively, and H_{eq} is a mass height from the base of foundation. As for the input motions, the translational and rocking motions observed on the basement of the building are used in the response analysis.
The composite acceleration response spectra in the NS direction for the input motions observed at the Tohoku Earthquake in 2011 are shown in **Figure 4.6** for two different mass heights. The case of H_{eq}=0 corresponds to the case when the rocking component of input motion is not taken into account, and H_{eq}=28.2m is chosen considering the effective height computed for the base-fixed fundamental mode of superstructure being about 20m above the ground in both directions. In these figures, the conventional response spectrum for the free field motions at the site is also shown for comparison. In the numerical computation, 3% of damping factor is assumed.
It may be observed from the results that for periods more than 1sec the response spectra are almost identical irrespective of different equivalent height, and the response to the effective input motions is almost same as the response to free field motion. These tendencies indicate that the effect of rocking input motion becomes small for structures with longer period more than 1sec. It is also noted that the response to effective input motions including the effect of rocking motion is less than the response to free-field motion. In addition, it might be important to note that the rocking input motion tends to increase the response of structures with shorter period less than 0.5sec.
In **Figure 4.7**, the averages of the response spectrum ratio between the composite spectrum and the response to only horizontal input motions are shown for the respective phases. Illustrated is result in

the NS direction. Clear distinction between different phases may be seen around periods between 0.4 and 1.2sec. The peak values observed around the periods tend to shift to the side of longer period and the peaks of the spectral ratio tend to get smaller as the phase shifts from one to four.

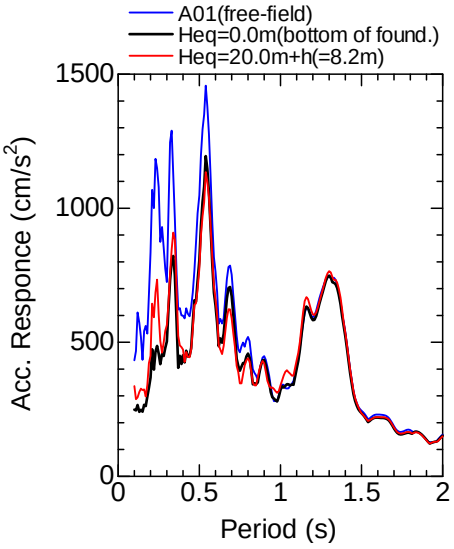

Figure 4.6. Composite response spectrum for the Tohoku Earthquake.(H_{eq} =0 & H_{eq}=28.2m)

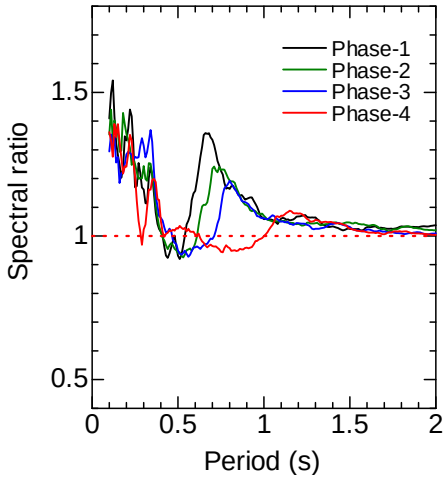

Figure 4.7. Response spectrum ratios of composite spectra to horizontal input motions

4.7 Temporal Variation of EIM during the Tohoku Earthquake in 2011

It would be interesting to observe the temporal variation of effective input motions during an extensive earthquake motion. **Figure 4.8** shows the time histories of horizontal and rocking EICs in the NS direction for the main and successively occurred aftershocks during the Tohoku Earthquake. In the figure, a time history of equivalent frequency of ground motion computed based on Eqn. (4.1) with shifting T_p by 4sec is shown together with the variation of instantaneous power of free-field motion.

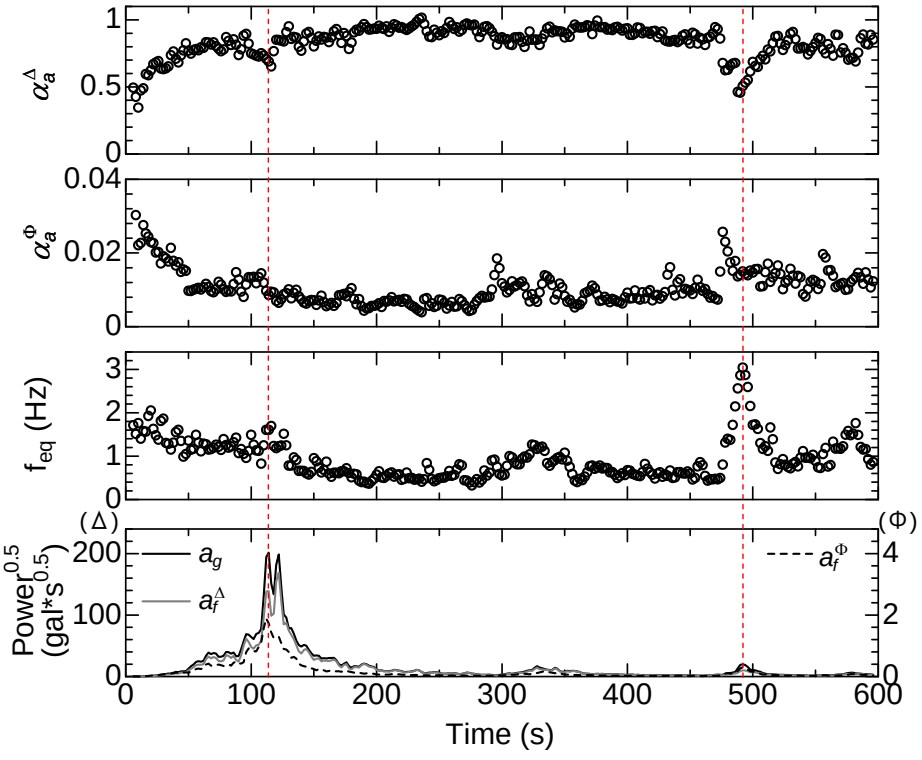

Figure 4.8. Temporal variation of EICs, f_{eq} and instantaneous power of the ground motion (NS component)

Inspecting the results shown in **Figure 4.8**, it may be observed that the translational effective input motion tends to increase and, in contrast, the rocking component to decrease associated with the decrease of predominant frequency as being detected with the passage of time. The most notable aspect in the results is sharp peaks of the EICs seen around 500sec at which the translational component of EIM drops drastically and the rocking component increases at time prior to the peak of translational input motion. The sudden degrease of translational component is due to increase of higher frequencies including in the ground motion as being depicted in the figure. The increase of rocking component, on the other hand, is seen at the time of a small power of ground motion. Thus, the cause of the emergence of the peak may be attributed to the small value of denominator in evaluation of the rocking component of EIC defined by Eqn. (3.2).

5. CONCLUSIONS

On basis of many earthquake records observed in a densely instrumented building and at the site for about 14 years, effective input motions to the superstructure were isolated and analyzed with focussing on a variation of characteristics of effective input motions over years. The lateral stiffness of the building has been deteriorating ever since it had completed, and taking advantage of the change in dynamic characteristics the effect of stiffness of superstructure on the effective input motion was studied. Main findings obtained through the study can be summarized as follow.

The variation of stiffness of superstructure affects especially on the rocking component of effective input motions, and little on the translational component. The rocking effective input motion tends to be pronounced for short-period structures. The effectiveness of the evaluation indices for effective input motions defined by Eqns. (3.1) and (3.2) was confirmed in this paper.

REFERENCES

Housner, G. W. (1957). Interaction of building and ground during an earthquake. *Bull. Seism. Soc. Am.* **47:3**, 179-186.

Yamahara, H. (1970). Ground motions during earthquake and input loss of earthquake power to an excitation of building. *Soils and Foundations*. **10:2**, 145-161.

Yasui, Y., Iguchi, M., Akagi, H., Hayashi, Y. and Nakamura, M. (1998). Examination on effective input motion to structures in heavily damaged zone in the 1995 Hyogo-Ken Nanbu Earthquake, *J. Struct. Constr. Engng*, AIJ, **512**, 111-118.

Iguchi, M., Unami, M., Yasui, Y. and Minowa, C. (2000). A note on effective input motions based on earthquake observations recorded on a large scale shaking-table-foundation and the surrounding soil, *J. Struct. Constr. Engng*, AIJ, **537**, 61-68.

Kojima, H., Fukuwa, N. and Tobita, J. (2005). A study on input loss effect of low and medium-rise buildings based on seismic observation and microtremor measurement, *J. Struct. Constr. Engng*, AIJ, **587**, 77-84.

Stewart, J. P., Seed, R. B. and Fenves, G. L. (1999). Seismic soil-structure interaction in buildings. II: Empirical findings, *J. Geotech. and Geoenvir. Engrg.*, ASCE, **125:1**, 38-48.

Kawashima, M., Iguchi, M. and Minowa, C. (2007). Extraction of effective input motions to structures based on earthquake observations and a measure for the input motions, *J. Struct. Constr. Engng*, AIJ, **615**, 85-92.

Kashima, T. and Kitagawa, Y. (2006). Dynamic characteristics of a building estimated from strong motion records using evolution strategy, *J. Struct. Constr. Engng*, AIJ, **602**, 145-152**.**

Iguchi, M., Kawashima, M. and Kashima, T. (2010). Assessment of varying dynamic characteristics of a SFSI system based on earthquake observation, *Workshop on Soil-Foundation-Structure Interaction* (Auckland, NZ), Soil-Foundation-Structure Interaction, ed. by Orense, Chouw and Pender, CRC Press, 3-10.

Harada, T., Kubo, K. and Katayama, T. (1985). Model of the effective seismic motions of embedded foundation and its verification by observed data. *Journal of Structural Mechanics and Earthquake Engineering*, JSCE, **362:I-4**, 435-440.

Subcommittee of Earthquake Engineering in Japan Society of Civil Engineering, (1992). *Dynamic interaction of Foundation-soil-structure system, - Introduction of interaction effect into seismic design* -, JSCE.

Kawashima, M., Nagano, M., Kashima, T. and Iguchi, M. (2012). Long- and short-term stiffness deterioration with aging for damage estimation in a building based on earthquake observation records, *Journal of Japan Earthquake Engineering*, (in press).